Two-dimensional condensed phases from particles with tunable interactions

Michael B. Hay,[1,*] Richard K. Workman,[2] and Srinivas Manne[1,†]
[1]*Department of Physics, University of Arizona, Tucson, Arizona 85721*
[2]*Department of Materials Science & Engineering, University of Arizona, Tucson, Arizona 85721*
(Received 7 March 2002; published 31 January 2003)

We present a conceptually simple experimental model for condensed phases, consisting of an ensemble of identical magnetic dipoles on a vibrating bed. The model combines tunable and accurately known pair potentials, equilibration times of seconds, and lattice structure and dynamics visible to the naked eye. Fundamental ensemble properties—specifically phonon propagation, edge relaxation, and binary condensation—are directly observed and quantitatively linked to the underlying pair potential.

DOI: 10.1103/PhysRevE.67.012401 PACS number(s): 64.60.−i, 61.25.−f, 62.65.+k

In ordinary solids, the connection between atomic interactions and bulk material properties is obscured because interatomic potentials generally cannot be derived *ab initio*, or measured in isolation, or varied externally. Several types of condensed matter analogs—ensembles of particles with soft and tunable interactions—have been used to bridge this gap. Macroscopic models have employed capillary forces between bubbles [1], magnetic forces between permanent magnets floated at liquid surfaces [2–7], and electrostatic forces between charged spheres [8,9] to form two-dimensional ordered phases. At the mesoscopic scale, colloidal crystals [10,11] have been prepared from charge-stabilized [12,13], polymer-stabilized [14], and paramagnetic [15–18] particles. Interaction tuning has been accomplished by variable external fields [6,18], which have served as a (reciprocal) pseudotemperature in phase transition studies [16,17].

Despite these successes, the quantitative link between pair potentials and material properties remains largely incomplete, for several reasons. Charge-stabilized colloids and macrospheres have exhibited unexpected long-range attractions [9,19,20], and the actual pair potential for these systems is now a matter of some uncertainty [11,21,22]. Most condensed matter models employ liquid media, which are associated with slow transport, long equilibration times (days to weeks for colloidal crystals), and lattice dynamics dominated by viscous drag and ion diffusion [23–25]. Although qualitative observations of edge relaxation [5,6,17] and binary condensation [7,26] have been reported, these structures have not been quantitatively linked to the underlying interactions. Extensive interaction-property relationships have been found only for hard-sphere systems [27], which lack a continuously tunable interaction.

We present a tunable, macroscopic, and solvent-free model system for condensed phases and report results for phonon propagation, edge relaxation, and binary condensation that correlate well with simple theoretical calculations. The apparatus (Fig. 1) consists of a large number $[(1-3)\times 10^3]$ of identical chrome steel spheres of radius R, confined to a finite planar area and subjected to a spatially uniform magnetic field B_0 directed normal to the plane [28]. Spheres separated by a center-to-center distance r repel via the dipole–dipole interaction,

$$w(r)=\frac{K}{r^3}\left(K\equiv\frac{4\pi}{\mu_0}B_0^2R^6\right). \tag{1}$$

Here B_0 is, strictly speaking, the *local* field at each dipole and is slightly smaller than the external field due to the opposing dipole fields of neighboring spheres; this field correction can be made self-consistently and is around 10% for typical lattices. For experimental convenience, the external field was a sinusoidal ac field generated by connecting the coils to line voltage (120 V, 60 Hz) through a variac. Equation (1) holds also for ac fields, provided $w(r)$ is the interaction averaged over one cycle and B_0 the root-mean-square value of the field. The additional moment due to Faradaic induction is $\sim 10^{-5}$ times the directly induced moment and can, therefore, be neglected.

The sample plate could be horizontally vibrated using an asymmetrically loaded, variable-speed dc fan (Fig. 1) whose rotation rate controlled the vibration amplitude [8]. This served as a crude but independently variable temperature that could be tuned to quickly anneal an ensemble to equilibrium, or, at higher amplitude, to melt the equilibrium structure. Although vibration annealing was usually unnecessary for

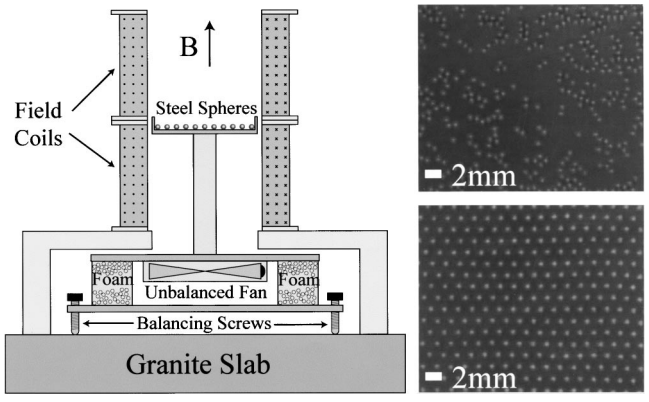

FIG. 1. (Left) Schematic of experimental apparatus. (Right) Self-organization of a random ensemble of spheres (top) in the presence of a magnetic field (bottom).

*Present address: Department of Civil & Environmental Engineering, Princeton University, Princeton, NJ 08544.
†Corresponding author.
Email address: smanne@physics.arizona.edu

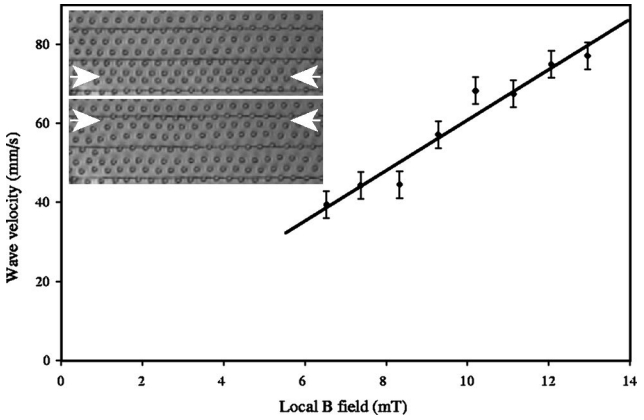

FIG. 2. Propagation speed of longitudinal phonons through the dipole lattice ($a=1.66$ mm) as a function of the local field (corrected for the opposing fields of the dipole lattice). The video frames (inset) show a sample longitudinal wave (arrows) that travels 5.6 mm in 67 ms [30].

the formation of pure lattices, it often proved useful for the condensation of binary phases, which exhibit higher kinetic barriers.

The pair potential [Eq. (1)], repulsive at all separations, caused initially random ensembles of spheres to expand rapidly outward to fill the bounding area (Fig. 1). For fields large enough to overcome the small frictional forces between the spheres and the flat plate, the dipoles ordered into a periodic lattice. In accordance with the inverse-cube interaction [29], observed dipole lattices were always triangular, independent of the field strength and the shape of the plate boundary. While *all* boundaries gave rise to triangular lattices, hexagonal boundaries proved most useful for promoting the rapid coalescence of single-domain, defect-free lattices.

Once a lattice was established, lightly tapping the supporting table produced longitudinal phonons whose propagation could be directly visualized (see Fig. 2 inset and supplementary video sequence [30]). The ''sound speed'' could be controlled by the applied field B_0 through its effect on the pair potential, Eq. (1). For a square lattice (considering only nearest-neighbor interactions), the sound speed $v_{square}=a\sqrt{k/M}$, where M is the mass and k is the stiffness of an atom in its equilibrium position with a single neighbor. For the triangular lattice of rolling spheres, this is modified to $v=a\sqrt{\sqrt{3}k/M^*}$, where the $\sqrt{3}$ factor comes from the lattice symmetry and $M^*\equiv 7M/5$ is the effective mass due to rolling motion. The stiffness can be directly calculated from the known pair potential [Eq. (1)], with the result $k=12K/a^5=(48\pi/\mu_0)B_0^2R^6/a^5$ [31]. Therefore, the sound speed for a given dipole lattice should vary linearly with the applied field:

$$v=\sqrt{\frac{48\sqrt{3}\pi R^6}{\mu_0 M^* a^3}}B_0. \tag{2}$$

Measured values of v vs B_0 (Fig. 2) confirm the expected linear trend, and the measured slope of 6.4 ± 0.6 m/T s is

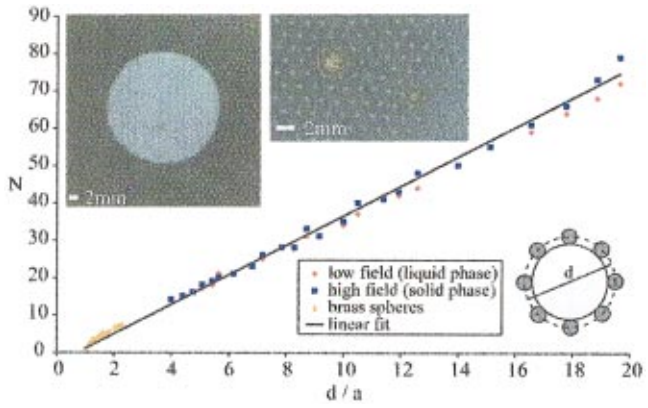

FIG. 3. (Color) Edge relaxation of the dipole lattice around nonmagnetic holes, ranging from large plastic discs to small brass spheres (top insets). The ''solvation number'' N is plotted vs the ratio d/a, where d is the diameter of the solvation shell (bottom inset). Similar values of N are obtained for both high field (squares) and low field (diamonds), the latter corresponding to the melting transition.

fairly consistent with the theoretical value of 7.9 m/T s. The difference is attributed to small frictional forces.

Knowledge of the pair potential also enables the prediction of lattice relaxation at a boundary edge. In real solids, the bulk exerts a net inward attraction on the surface layer, causing a compression of surface bonds and leading to a higher atomic density at the surface. The dipole lattice shows a similar higher density of magnetic spheres near a nonmagnetic boundary. While this effect is readily observed at the outer plate boundary, it is better quantified at inner boundaries created by nonmagnetic ''holes,'' ranging in size from large plastic discs to small brass spheres (Fig. 3, top insets).

A simple analytical expression for the edge relaxation is found by considering a bulk lattice half plane of lattice constant a terminated by a single edge layer of lattice constant a' and equating the chemical potentials μ_{bulk} and μ_{edge}. Because the edge relaxation is independent of temperature (see below), the entropic contribution is negligible, and μ_{bulk} is the Madelung sum of inverse-cube interactions over a two-dimensional triangular lattice,

$$\mu_{bulk}(a)=K\sum_{\text{lattice}}\frac{1}{r_i^3}\equiv C\frac{K}{a^3}. \tag{3}$$

Here $C\approx 10.95$ is the Madelung constant for a triangular lattice, calculated numerically. Similarly, for a dipole in a single *isolated line* of dipoles with lattice constant a',

$$\mu_{line}(a')=K\sum_{n=1}^{\infty}\frac{2}{(na')^3}\equiv C'\frac{K}{a'^3}, \tag{4}$$

where $C'\approx 2.40$ is Madelung constant for an isolated line. In the hypothetical case of a simple bulk termination (i.e., a semi-infinite lattice of lattice constant a), the chemical potential of a particle at the edge would be $\frac{1}{2}\mu_{bulk}(a)+\frac{1}{2}\mu_{line}(a)$. However, because the edge spacing is a',

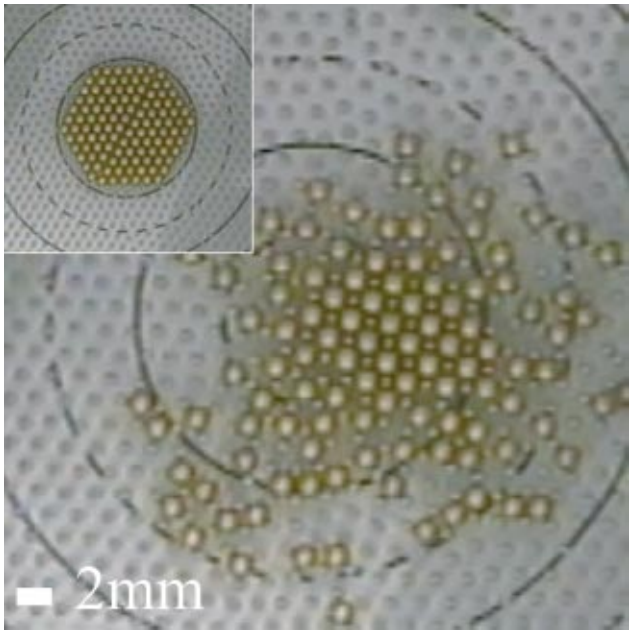

FIG. 4. (Color) Binary condensation from a mixture of dipoles (steel spheres) and holes (brass spheres) favoring $N=4$ ($a=1.66$ mm and $d=2.25$ mm). The ensemble is initially prepared with the brass spheres close packed at the center. (inset) Under moderate vibration (insufficient to melt the lattice), the dipoles solvate the holes and eventually establish a dynamic equilibrium between "dissolved" holes and a four-coordinated binary condensate [30]. (The black circles in the figures are calibration marks and can be ignored.)

$$\mu_{edge}=\left[\frac{1}{2}\mu_{bulk}(a)+\frac{1}{2}\mu_{line}(a)\right]-\mu_{line}(a)+\mu_{line}(a')$$

$$=(C-C')\frac{K}{2a^3}+C'\frac{K}{a'^3}. \tag{5}$$

Equating μ_{edge} to μ_{bulk} [Eq. (3)] finally gives

$$a'=\sqrt{\frac{2C'}{C+C'}}\ a\approx 0.71a. \tag{6}$$

The assumption of a single relaxed edge layer, therefore, predicts a 29% decrease in the edge spacing, independent of the applied field.

This prediction is tested by counting the number N of dipoles that spontaneously surround nonmagnetic holes of varying size placed in lattices of varying a. Letting d be the diameter of the solvation shell around a hole (Fig. 3, bottom inset) and using Eq. (6) gives,

$$N=\pi d/a'\approx 4.42(d/a). \tag{7}$$

The measurements of N vs d/a (Fig. 3) show a clear linearity over a wide range of d and a. Observed values of N are independent of the external field, even down to values of B_0 small enough to melt the lattice, therefore justifying the assumed temperature independence. The measured dimensionless slope of 4.0 ± 0.2 is in reasonable agreement with Eq. (7), considering the simplifying assumptions of an infinite linear edge and relaxation limited to a single layer. The first assumption in particular is justified only when $d\gg a$, so it is surprising that the linearity approximately holds even for smaller holes such as the brass spheres.

The high-density "adsorption" of dipoles onto small holes (e.g., Fig. 3) suggests an analogy to solvation shells of a continuous phase (dipoles) around discrete solutes (holes), with N serving as the solvation number. As the solute concentration is increased, the attractive hole-dipole interaction should favor binary condensation of holes and dipoles in a mixed phase. Real-world analogues include hydrated crystals from solutions and stoichiometric alloys from miscible melts. Although binary phases have been reported for both charge-stabilized and paramagnetic colloid mixtures [18,26], there exists no quantitative prediction of these structures based on pair potentials. Our experiments with mixed ensembles showed that the solvation shell of the dissolved phase served as a simple predictor for the structure and stoichiometry of the condensed binary phase.

A typical experiment is initially prepared with the brass spheres artificially segregated from the steel spheres [Fig. 4(inset)]. The size of the brass spheres and the density of the steel spheres are chosen for a specific d/a ratio, which in turn selects for a specific solvation number via Fig. 3. For the conditions of Fig. 4, the optimum solvation number $N=4$. With the vibration off, the dipole lattice and the close-packed holes remain phase segregated indefinitely. Under low vibration (below the melting transition of the dipole lattice), the dipoles begin to infiltrate and solvate the nonmagnetic cluster. Some holes dissolve and escape, while others rearrange into a new condensate to accommodate the dipoles, eventually (in ~ 100 s) resulting in an ordered binary lattice coexisting with a gas phase of solvated holes [Fig. 4]. The size of the condensate decreases with increasing vibration amplitude, until at high vibration only a gas phase of solvated holes remains.

Binary condensates such as Fig. 4 display several interesting properties. The phase coexistence with solvated holes shows that condensation comes from *cohesive* (attractive) interactions between solvated holes, in contrast with the repulsive interactions of the pure dipole lattice. The solvation number (four) of the gas phase matches the coordination number (four) of the solid phase, leading to the final ordered structure of interpenetrating square lattices of dipoles and holes. This coordination number in turn fixes the stoichiometry of the binary phase to D_1H_1, where D is the dipole and H the hole. The free surfaces of the binary lattice show greater mobility than the bulk binary phase, in analogy with premelting of free surfaces observed in real solids. Finally, binary lattices often nucleate at and grow inward from a boundary wall, again in analogy with heterogeneous nucleation at solid surfaces. Many of these features are visible in the video sequence available as supplementary material [30].

Changing the initially chosen value of d/a selects for a different solvation number and therefore a different coordination and stoichiometry of the binary condensate. Increasing the solvation number to six, for example, can be accomplished either by reducing a [Fig. 5(a)] or by increasing d

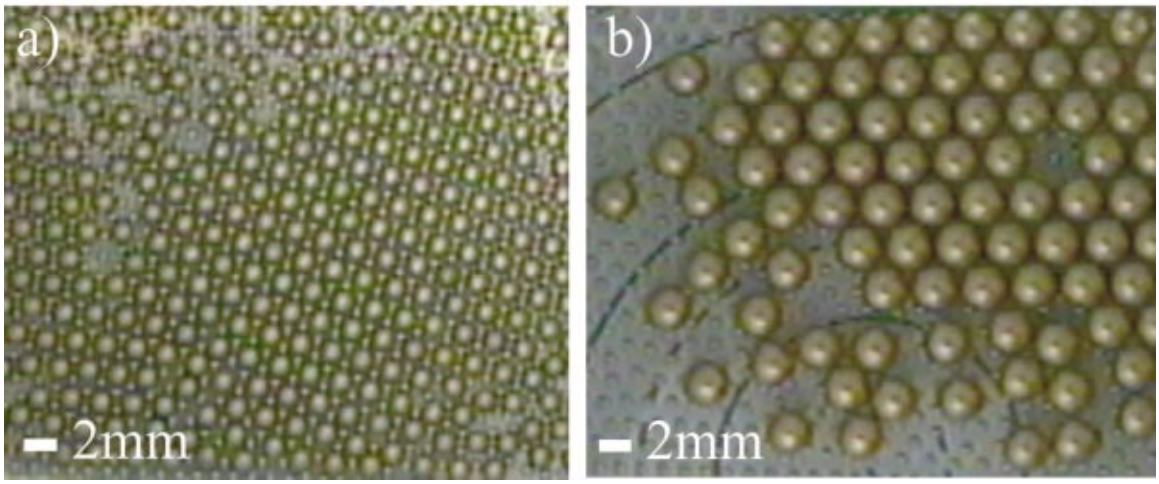

FIG. 5. (Color) Binary condensates under conditions that favor N=6. In (a), the ensemble was prepared with a=1.38 mm and d =2.25 mm, whereas in (b), the choices were a=1.66 mm and d=3.17 mm. In both cases, dipoles are six-coordinated to holes, resulting in a triangular lattice of holes interlaced by a honeycomb lattice of dipoles. (The latter is not readily visible in (b), where the steel spheres are mostly hidden by the much larger brass spheres.) Solid grains of the binary phase coexist with free solvated holes, and stable voids are visible. (The black arcs are calibration marks and can be ignored.)

[Fig. 5(b)]. In both cases, the binary condensate shows holes six-coordinated to dipoles, resulting in a triangular lattice of holes interlaced by a honeycomb lattice of dipoles. The resulting stoichiometry is now D_2H_1. Square lattices are never observed for systems whose optimum solvation number is six, just as hexagonal lattices are never observed for systems whose optimum solvation number is four.

That the same sizes of steel and brass spheres can lead to different binary structures [compare Figs. 4 and 5(a)] shows that the structures are *not* caused by geometric packing effects. Rather, the structure of the binary condensate depends on the details of the interaction potential, via the lattice relaxation calculations and measurements. This quantitative link between solvation and coordination numbers suggests a simple way to predict binary colloidal structures and to select for specific binary architectures in photonic band-gap materials.

We thank C. A. Stafford and R. E. Goldstein for useful discussions and G. G. Warr for the demonstration of a hard-sphere vibrating bed which served as the inspiration for this work. We gratefully acknowledge support from the National Science Foundation and from the Van de Verde Undergraduate Research Endowment.

[1] L. Bragg and J.F. Nye, Proc. R. Soc. London, Ser. A **190**, 474 (1947).
[2] A.C. Rose-Innes *et al.*, Cryogenics **9**, 456 (1969).
[3] H. Meissner and P. Crowley, Cryogenics **12**, 91 (1972).
[4] P.H. Melville and M.T. Taylor, Cryogenics **10**, 491 (1970).
[5] P.H. Melville, J. Mater. Sci. **10**, 7 (1975).
[6] M. Golosovsky *et al.*, Appl. Phys. Lett. **75**, 4168 (1999).
[7] Y. Saado *et al.*, Synth. Met. **116**, 427 (2001).
[8] B. Pouligny *et al.*, Phys. Rev. B **42**, 988 (1990).
[9] B.V.R. Tata *et al.*, Phys. Rev. Lett. **84**, 3626 (2000).
[10] P. Pieranski, Contemp. Phys. **24**, 25 (1983).
[11] A.K. Arora and B.V.R. Tata, Adv. Colloid Interface Sci. **78**, 49 (1998).
[12] R.S. Crandall and R. Williams, Science **198**, 293 (1971).
[13] C.A. Murray *et al.*, Phys. Rev. Lett. **58**, 1200 (1987).
[14] A.H. Marcus and S.A. Rice, Phys. Rev. Lett. **77**, 2577 (1996).
[15] A.T. Skjeltorp, Phys. Rev. Lett. **51**, 2306 (1983).
[16] K. Zahn *et al.*, Phys. Rev. Lett. **82**, 2721 (1999).
[17] R. Bubeck *et al.*, Phys. Rev. Lett. **82**, 3364 (1999).
[18] W. Wen *et al.*, Phys. Rev. Lett. **85**, 5464 (2000).
[19] N. Ise *et al.*, J. Chem. Phys. **78**, 536 (1983).
[20] J.C. Crocker and D.G. Grier, Phys. Rev. Lett. **77**, 1897 (1996).
[21] T.M. Squires *et al.*, Phys. Rev. Lett. **85**, 4976 (2000).
[22] R. Messina *et al.*, Phys. Rev. Lett. **85**, 872 (2000).
[23] A.J. Hurd *et al.*, Phys. Rev. A **26**, 2869 (1982).
[24] B.U. Felderhof and R.B. Jones, Z. Phys. B: Condens. Matter **64**, 393 (1986).
[25] M. Hoppenbrouwers and W. van de Water, Phys. Rev. Lett. **80**, 3871 (1998).
[26] S. Hachisu *et al.*, Nature (London) **283**, 188 (1980).
[27] A. Imhof and J.K.G. Dhont, Phys. Rev. Lett. **75**, 1662 (1995).
[28] Chrome steel precision ball bearings of radius 397 ± 1 μm and mass 2.04 mg were obtained from Small Parts, Inc.
[29] Due to the centrosymetric pair potential, we expect lattices with high symmetry, i.e., triangular or square. For a fixed particle density, the Madelung sum is 1.04 times larger for a square lattice than for a triangular lattice.
[30] Supplementary video clips can be found at http://www.physics.arizona.edu/~smanne/MagneticSpheres/magspheres.html.
[31] Our values of k typically fell in the range 10^{-4} to 10^{-3} N/m, corresponding to lattice bulk moduli of order $k/a\sim1$ Pa, comparable to those of charge-stabilized colloids [12].